ORIGINAL PAPER

Comparison of atmospheric turbulence characteristics and turbulent fluxes from two urban sites in Essen, Germany

Stephan Weber · Klaus Kordowski

Abstract From September 2006 to September 2007, the intersite variability of turbulence characteristics and turbulent heat fluxes was analysed at two urban stations in Essen, Germany. One site was situated within an urban residential setting while the other was located at the border of an urban park and suburban/urban residential housing. Therefore, the surroundings at both sites contributing to surface–atmosphere exchange differed in terms of surface cover and surface morphology. During the 1-year measurement period, 19% of data were characterised by stable atmospheric stratification. Since observations of urban turbulence characteristics under stable stratification are scarce, so far, this work adds additional input to this discussion. Turbulence characteristics, i.e. normalised standard deviations of wind components, were in agreement to empirical fits from other urban observations under both instable and stable atmospheric stratification. However, differences in magnitude of turbulence characteristics between sites were observable. Comparison of turbulent heat fluxes indicated typical urban features in the site located in the urban setting with increased surface heating and higher surface heat fluxes by about 30%. Also the temporal evolution of heat fluxes on the diurnal course was affected. Differences in momentum flux were of minor magnitude with about 6% variation on average between sites. Findings indicate that multiple urban flux measurements within one city may be characterised by general similarities in terms of turbulent characteristics but are still significantly influenced by differences in the surface cover of the flux footprint.

S. Weber (✉) · K. Kordowski
Department of Applied Climatology and Landscape Ecology,
Institute of Geography, University of Duisburg—Essen,
Campus Essen,
45127 Essen, Germany
e-mail: stephan.weber@uni-due.de

K. Kordowski
e-mail: klaus.kordowski@uni-due.de

1 Introduction

The turbulent atmosphere–surface exchange in urban areas is significantly modified from the nonbuilt surrounding (Oke 1988; Roth 2000; Kuttler 2008). This is due to the degree of urban complexity, e.g. various artificial and natural surface covers, large number of roughness elements, and emission of anthropogenic heat. Those parameters significantly affect urban microclimates and the dispersion of pollutants in the urban boundary and canopy layer (Weber et al. 2006; Weber and Weber 2008).

At present, more than 50% of the world's population live in urban agglomerations with more than 70% to be reached in the course of the 21st century (Arnfield 2003; UN-Habitat 2006). To better manage air and environmental quality in cities, an increased understanding of the exchange of heat, mass, and momentum between the atmosphere and the urban surface is necessary. However, the number of urban turbulence data sets (i.e. turbulence characteristics, atmospheric stability, heat and momentum fluxes) is scarce or limited to short periods of time not covering different seasons and meteorological conditions.

In recent years, a number of turbulent flux measurements were performed in cities around the globe, most of them focusing on the urban surface energy balance (e.g. Oke et al. 1999; Spronken-Smith 2002; Nemitz et al. 2002; Christen and Vogt 2004; Offerle et al. 2006; Newton et al. 2007; Vesala et al. 2008). Measurements are generally installed at some height above the city, i.e. within the inertial sublayer (constant flux layer) at 1.5 to five times the

mean building height. The structure of atmospheric turbulence has shown to be rather homogeneous in this region when the flow has adjusted to the underlying surface (Roth 2000). However, most of the studies are restricted to single flux measurement sites to characterise the urban surface–atmosphere exchange. Hence, the resulting information is limited to a section of the surface contributing to the turbulent flux (the so-called flux footprint) which depends on the measurement height above ground level, atmospheric stability, and the intensity of crosswind turbulence (Schmid 1997). This might somehow limit the spatial representativeness of single flux measurements sites in urban areas.

Some groups used multiple towers in field or wind tunnel experiments to study the spatial variability of urban boundary layer turbulence (Kastner-Klein and Rotach 2004; Christen and Vogt 2004; Kanda et al. 2006). In Marseille, flux measurements were performed at two different heights above roof top to verify the representativeness of fluxes (Grimmond et al. 2004). Depending on the measurement height above ground level, momentum flux between both measurement heights differed by about 20%, sensible heat flux by up to 80% (Grimmond et al. 2004). Differences were mainly related to the lower measurement height being not located within the constant flux layer. Surface energy balance measurements at two dense urban sites in Basel separated horizontally by about 1.5 km showed good agreement in terms of measured turbulent heat fluxes (Christen and Vogt 2004; Rotach et al. 2005). On the annual basis, daytime energy partitioning into sensible and latent heat was nearly similar (Christen and Vogt 2004). In Tokyo, five towers were set up in an area of ≈2 km^2 to estimate the spatial variation of roughness sublayer fluxes (Kanda et al. 2006). The authors demonstrated differences for time-averaged turbulence statistics of about 5% (standard deviation of vertical wind speed σ_w), 17% (friction velocity u_*), and up to 20% (sensible heat flux Q_H) during daytime.

There is still some discussion about the characteristics of atmospheric stability in urban boundary layers tending to show a high percentage of neutral and unstable stratification. Even the nocturnal urban boundary layer was reported to remain unstable or neutrally stratified due to the release of stored heat from the urban fabric (e.g. Grimmond and Oke 2000; Arnfield 2003; Grimmond et al. 2004). However, those findings were mainly based on short-term observational periods carried out during summertime.

The motivation of this study is to compare conditions of atmospheric stability, turbulence characteristics and turbulent fluxes of heat, and momentum from two measuring sites within one city separated by a horizontal distance of about 5.5 km. The sites are different in terms of surface cover, surface morphology, and roughness. The question

arises to what extent fluxes and turbulence characteristics will differ between sites. This will prove important if data is used as an "urban estimate" in applications such as dispersion modelling of urban air pollutants.

The data analysis will be based on a 1-year data set covering different meteorological conditions to compare the seasonal variation in turbulence between sites.

2 Study sites

A 1-year turbulence data set was collected at two sites in Essen, Germany, in the time period from September 15, 2006 to September 15, 2007. Essen (585,000 inhabitants) is situated in the western part of Germany and covers a surface area of about 210 km^2.

The first site was installed in an urban surrounding (URB) in the northern part of the city (Figs. 1 and 2). A sonic anemometer was mounted at a height of $z=35$ m above ground level (agl). The 10 m mast erected on a rooftop had a diameter of 0.1 m. The building itself has a height of 25 m agl and is one of the largest in this area. The flat surrounding comprises of residential buildings of three to five floors. A mean building height of about $z_H=17$ m
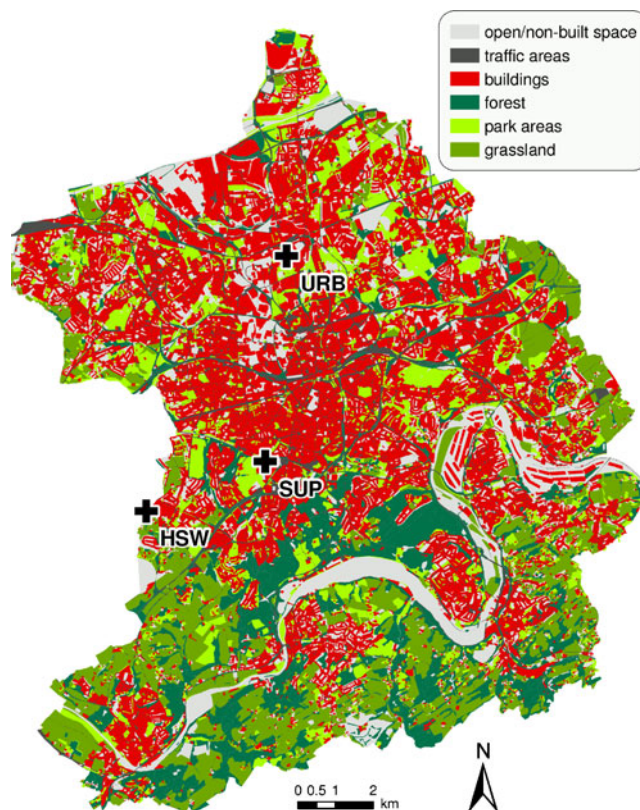

Fig. 1 Classification of land use types within the city boundaries of Essen, Germany. Measurement sites URB and SUP are depicted by *black crosses*. *HSW* indicates the rural station Harscheidweg

Fig. 2 Land use classification (*top*) and aerial photographs (*bottom*) for both flux measurement sites. A surface area with a radius of 1 km was taken into account for surface analysis (cf. Table 1)
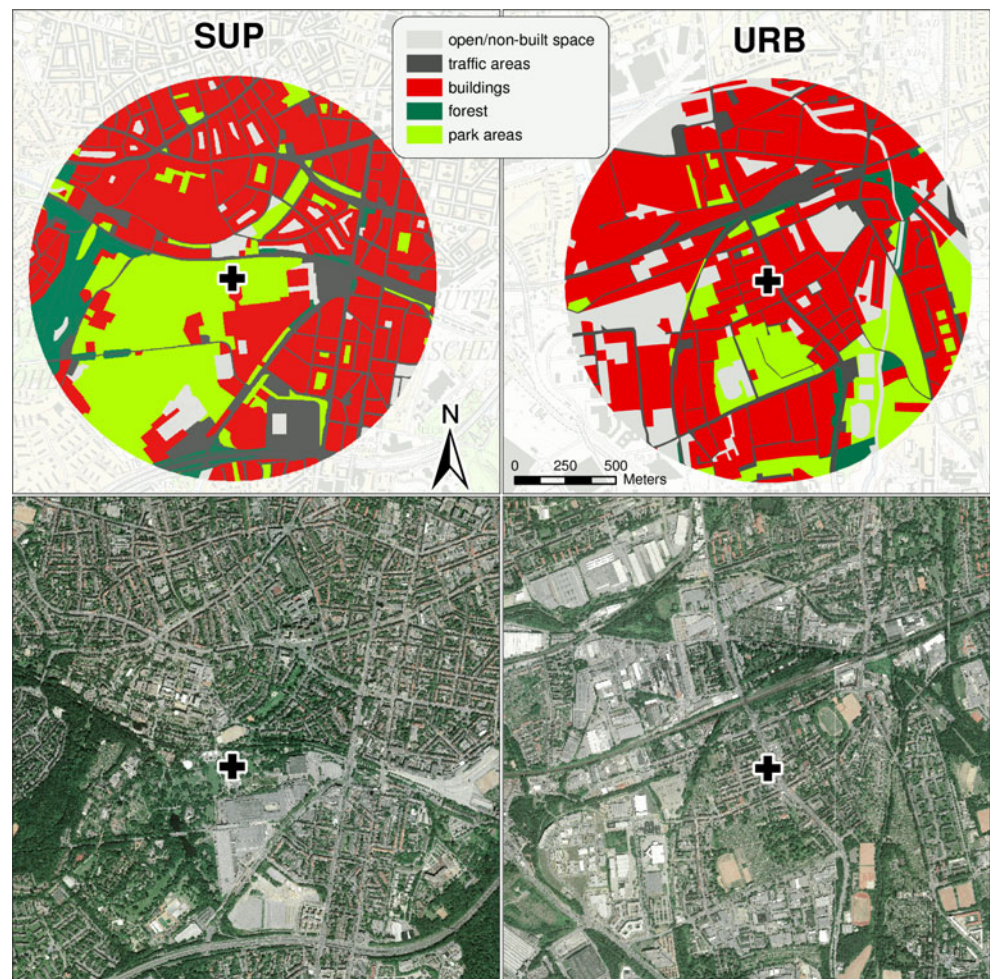
was estimated for this area of the city based on a data product from aerial laser scans provided by the city of Essen (cf. Table 1 for details). The sonic anemometer at this site was maintained by the North-Rhine Westphalia State Agency for Nature, Environment, and Consumer Protection.

The second site (SUP) was installed in the southwestern part of Essen at the border of an urban park in the southwest of the station and suburban/urban residential areas to the north and east with buildings of two to four floors (cf. Figs. 1 and 2). The southeast is characterised by exhibition areas with some larger buildings. The main exhibition centre (mean height≈15 m) is situated at a distance of about 150 m to the south/southeast of the measurement site (Fig. 2). A solid concrete tower— basically a visitor attraction and observation tower of the park—hosted the measurements. From a platform at a height of 26 m agl, a horizontal boom hosting the sonic was extending about 3.5 m from the tower to the southeast facing 150°. The urban park located in the southwest of the measurement site covers a surface area of about 70 ha. The terrain negligible slopes by about 10 m over a distance of 400 m to the southwest, however, generally, the site can be

characterised as flat. Differences in surface characteristics around both sites will be assessed in Section 3.2.

3 Material and methods

3.1 Instrumentation

Both sites were equipped with sonic anemometer–thermometers (USA-1, Metek, Germany) sampling horizontal and vertical wind vectors u, v, w, and acoustic temperature (T_s) at a rate of 10 Hz. Five-minute block averages of u, v, w, T_s, and covariances were calculated from raw data and stored for subsequent analysis. The 5-min block averages were subjected to tests for implausible data, afterwards, 30-min averages were aggregated. For flux calculation, data were rotated into streamwise coordinates by a double-rotation procedure according to Kaimal and Finnigan (1994).

At URB, only 5-min block averages of turbulence data were stored; at SUP, also raw data were available. The possible underestimation of turbulent fluxes due to shorter averaging lengths (e.g. larger eddies might not be sampled

Table 1 Measurement heights and surface characteristics of both sites

Surface characteristics	SUP	URB
Station surroundings	Urban park, residential housing	Residential housing
z (m)	26	35
z_H (m)	15	17
z_0 (m)	1.24	1.18
d (m)	10.6	11.2
z/z_H	1.73	2.05
z/z_0	22.8	29.7
$\lambda_b(\lambda_b 180 < \phi < 270)$[a]	0.48 (0.14)	0.55 (0.51)
L (m)	520	700
$\sigma_v/u*$	1.50	2.06

The parameters z_0, L, and $\sigma_v/u*$ are mean values derived from the sonic anemometer measurements at the sites. z is the measurement height above ground level, z_H the mean building height, z_0 the aerodynamic roughness length, d the displacement height, and λ_b the plan area density for all wind directions ϕ (in brackets for wind direction sector $180 < \phi < 260$). L the Obukhov length, $\sigma_v/u*$ a measure for lateral turbulence intensity are parameters needed for the calculation of flux footprints for near-neutral conditions ($-0.05 < \zeta < 0.05$) according to Schmid (1994, 1997)

[a] Building plan area density: ratio of plan building area to plan area of total surface

sufficiently, e.g. Foken 2006) was estimated at SUP from a comparison of (1) the 30-min averaged fluxes from 5-min blocks and (2) 30-min averaged fluxes from raw data. Based on 1-year data, the mean underestimation is <10% for the momentum flux and <15% for sensible heat flux which we assume to be similar at both stations. However, since we were mainly interested in comparing the relative differences between the two sites, we consider the underestimation of absolute fluxes as acceptable within the scope of this paper. For subsequent analysis, 30-min turbulent fluxes at URB and SUP were calculated from 5-min block averages.

Due to interference and flow distortion by the tower at SUP data from a wind direction (ϕ) sector, $260° < \phi < 360°$ was rejected from data analysis at both sites.

Data storage failure at URB in the period from May 2 to 22, 2007 led to rejection of about 3 weeks of data at both sites. However, data availability (30 min averages) for the 1-year period accounts to 81%. The subsequent data analysis is based on a set of $n=14{,}153$ half-hourly means from both turbulence sites covering identical time periods.

To study effects of atmospheric stratification, the surface layer stability parameter $\zeta = (z - d)/L$, with d the displacement height in m, and L the Obukhov length in m was calculated. Displacement height was assumed as $d=0.66\,z_H$ (e.g. Garratt 1992; Grimmond and Oke 1999). With the estimated displacement height, the aerodynamic roughness length z_0 was evaluated anemometrically from measured

data using the log law of the vertical wind profile (cf. Table 1). Data in the range $-0.05 < \zeta < 0.05$ was defined as neutral atmospheric stratification.

In order to make kinematic heat fluxes, $\overline{w'T_s'}$ measured by eddy covariance comparable to sensible heat fluxes from other urban studies, i.e. urban energy balance studies, Q_H is estimated according to

$$Q_H = \rho c_p \overline{w'T_s'} \tag{1}$$

by assuming constant density of air ($\rho=1.2$ kg m^{-3} at 20°C) and specific heat capacity of air at constant pressure ($c_p=1005$ J kg^{-1} K^{-1}, e.g. Stull 1988). Assuming constant density of air throughout a 1-year study period will result in small inaccuracies in absolute fluxes due to air temperature differences, e.g. in comparison between summer and winter situations. However, the deviations are small (<3% at maximum) and thought to be negligible in the scope of this paper. However, for reasons of comparison, we will refer to both kinematic and sensible heat fluxes in subsequent data analysis.

To characterise ambient meteorology during the study period, data from the rural station Harscheidweg (HSW) at the western border of the city of Essen was used (Fig. 1). Air temperature (T_a, measured with Pt100, Friedrichs, Germany), relative humidity (RH, type 3112, Friedrichs, Germany), shortwave downward radiation (S_d, CMP11, Kipp&Zonen, Netherlands), and precipitation (P, type 7501, Friedrichs, Germany) were measured at 2 m agl (precipitation at 1 m agl) and recorded as 3-min averages and precipitation sums, respectively.

3.2 Surface characteristics around the measurement sites

To support interpretation of turbulent fluxes and turbulence characteristics from both measurement sites, differences in surface characteristics and surface morphology around both stations were assessed. The footprints contributing to the surface–atmosphere exchange were calculated by the model of Schmid (Schmid 1994; 1997) for neutral atmospheric stability. The footprint model was initialised with the measurement height agl, the aerodynamic roughness length, and average values for lateral turbulence intensity $\sigma_v/u*$ from our measurements (see Table 1 for model parameters).

For straightforward analysis of surface cover and different surface morphology in the flux source areas around both stations, the spatial domain was limited to a 1-km radius around the measurement sites. This represents a 60% to 70% flux source area for both sites under neutral stratification according to the footprint model. Land use was classified into the following six classes: open/nonbuilt spaces, traffic areas, buildings, forest, park areas, grassland (cf. Figs. 1 and 2).

On average, the fraction of surface cover is not significantly different, and plan area density at URB and SUP is about the same order (Table 2). Main differences are related to the percentages of open/nonbuilt spaces and park areas. The fraction of unsealed, vegetated surface at SUP with about 30% is roughly twice the amount in comparison to URB. However, when focussing on certain wind direction sectors, significant differences become evident. The southwest sector ($180° < \phi < 260°$) at SUP is mainly influenced by the urban park. The southwest is characterised by a park fraction of 58% (14% buildings) at SUP and a 50% building fraction (13% parks) at URB. In terms of surface roughness, this wind direction sector is dissimilar at both sites as indicated by a large difference in the value of λ_b (Table 1).

4 Results and discussion

4.1 Meteorological situation during the study period

The wind frequency distribution during the measurement campaign is comparable at both sites with a maximum from southwesterly/westerly directions (Fig. 3). With a wind direction frequency of 48% at URB and 56% at SUP in the sector $180° < \phi < 260°$, the wind direction was mainly from the southwest (park fetch at SUP, urban fetch at URB). Northwesterly directions are significantly underestimated at SUP due to shading by the tower construction (cf. Section 3.1). The yearly course of mean wind velocity is characterised by maxima during the winter period (November–January, Fig. 4a). The higher wind velocity at URB is due to the difference in absolute measurement height agl which is 9 m higher at URB.

Monthly averages of other meteorological quantities gathered at HSW are depicted in Fig. 4. The study period was characterised by an average air temperature of 12°C ($\pm$ 5.6°C standard deviation) and a precipitation sum of about 1,017 mm. Both are elevated in comparison to the long-term average of 9.6°C and 931 mm (period 1961–1990, German weather service station Essen, latitude 51° 24′ N, longitude 6° 58′ E; Müller-Westermeier 1996). The month of April 2007 was marked by a period of high surface pressure during easterly wind directions. Conditions were nonovercast mainly with high duration of sunshine. The monthly average shortwave downward radiation $S_d =$ 199 W m^{-2} is larger by about 20 W m^{-2} in comparison to the monthly average in May, June, or July (Fig. 4c). April 2007 was extraordinarily dry and warm. At HSW, only 0.2 mm of precipitation was recorded. Average T_a was 13.6°C which is 4.7°C above the long-term average (Müller-Westermeier 1996).

4.2 Atmospheric stability

Conditions of atmospheric stability have important implications for the dispersion of atmospheric pollutants. The frequency distribution of atmospheric stability measured during the 1-year period is depicted in Fig. 5. Similar to observations at other urban sites (e.g. Grimmond and Oke 2000; Grimmond et al. 2004; Christen 2005), the maximum of the frequency distribution of stability at both sites lies within the neutral range with about 44% of data at URB and 56% at SUP. The higher fraction of unstable situations at URB=31% (SUP=21%) is due to enhanced surface heating of artificial surface and roof materials in the vicinity of URB. This fact also becomes apparent in the average diurnal course of ζ indicating stronger instability at URB during daytime (Fig. 6). Note that, for characterisation of diurnal courses of ζ, the median value is plotted. Especially due to small nocturnal values of thermal $(\overline{w'T_s'})$ and mechanical (u_*) turbulence the resulting Obukhov length

Table 2 Overview of fraction of surface cover in a 1-km radius around both sites based on the six-class land surface cover classification

Surface cover	All wind directions		SW $180° < \phi < 260°$		NE $0° < \phi < 90°$	
URB	ha	%	ha	%	ha	%
Open/nonbuilt spaces	51.2	16.2%	20.0	25.4%	12.3	15.6%
Traffic areas	42.5	13.5%	8.4	10.6%	13.2	16.7%
Buildings	173.1	54.8%	39.9	50.6%	46.7	59.2%
Forest	7.4	2.3%	0.1	0.1%	3.3	4.2%
Park areas	41.5	13.1%	10.4	13.2%	3.3	4.2%
SUP						
Open/nonbuilt spaces	15.4	4.8%	5.2	6.5%	4.3	5.4%
Traffic areas	59.8	18.9%	7.0	8.8%	18.2	22.9%
Buildings	150.8	47.5%	11.1	14.0%	46.7	58.8%
Forest	17.9	5.6%	9.7	12.3%	0.8	1.0%
Park areas	73.4	23.1%	46.3	58.4%	9.4	11.8%

The class grassland does not exist in both 1-km circles

Fig. 3 Wind frequency distribution classified according to different wind speeds at both sites during the study period from September 2006 to September 2007. In this figure, all wind directions are included. Data is binned into 10°-classes
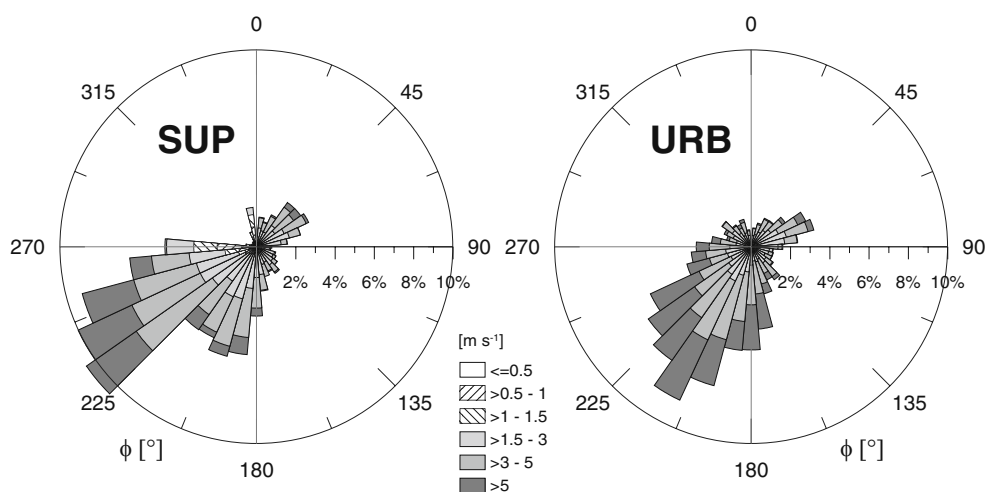
becomes large and biases the arithmetic mean of ζ (e.g. Mahrt et al. 1998). The median value therefore is a more robust estimate.

The majority of situations, about 81% at both sites, characterises nonstable atmospheric stratifications, i.e. $\zeta <$ 0.05. However, with the remaining $\approx$19% of data, a significant amount of stable stratification was measured. The diurnal course of ζ for the 1-year study period indicates nocturnal periods at both sites to be characterised by neutral situations mainly (Fig. 6, median $-0.05 < \zeta < 0.05$). However, a distinct fraction of data lies beyond the neutral stability criteria indicating stable situations at both sites starting from around 2100 Central European time (CET). The surface has sufficiently cooled by that time so that a change of sign in turbulent heat fluxes results in small but negative (downward) heat fluxes at night (this will be discussed in more detail in Section 4.4). Results from published literature generally illustrate small percentages of stable urban stratification. From a 4-week summer campaign in Marseille, France, Grimmond et al. (2004) reported only 1% of data being stable. In a 4-week summer campaign in Basel, Switzerland, only about 5% of nocturnal data from an urban measurement tower tended to be stable (Vogt et al. 2006). Generally, the urban heat island effect with release of stored heat from the urban fabric is believed to be responsible for unstable or neutral atmospheric stratification even during night time (Piringer et al. 2002; Arnfield 2003; Christen 2005). A compilation of flux measurements from ten North American cities indicates most of the sites to remain unstable/neutral during night (Grimmond and Oke 2000). However, comparability with our data is difficult since most of those campaigns were relatively short summer campaigns (<8 weeks), and study sites were distributed on more southern latitudes.

Although distinct seasonal variation can be observed in the diurnal courses of the stability parameter, the general behaviour of the two sites is preserved (Fig. 7). The largest amplitude in the diurnal course of stability at both sites is evident during the seasons characterised by stronger insolation and higher turbulent transport by convection (spring and summer seasons). However, those weather conditions with larger frequencies of clear and calm days also favour increased nocturnal cooling of the surface and a higher tendency towards stable stratification. Maximum positive values of ζ are therefore observed during the months March, April, and May (MAM, spring season) and June, July, and August (JJA, summer season, Fig. 7). The larger absolute value of ζ at URB during the MAM period is related to very calm periods during the month of April 2007. Similar but very small numbers of $\overline{w'T_s'}$ and u_* at both sites led to small numbers of L and therefore, due to a greater measurement height agl at URB, resulted in larger estimates of ζ. During the remaining season, nocturnal estimates of median ζ were similar.

It can be concluded that stability regimes at both urban sites are similar during nighttime but the higher percentage of artificial surface cover favours more frequent and stronger unstable situations at URB during daytime.

4.3 Turbulence characteristics

4.3.1 Surface roughness

As noted before, the fraction of surface cover around both sites is similar on average, however, distinct variability depending on the direction of flow can be observed (cf. Table 2). This will have impact on the intensity of turbulence created. The relation can be expressed by the drag coefficient C_D, defined as the square of the ratio of friction velocity and mean wind velocity (Roth 2000). Owing to the direction of approaching flow and differences in surface cover, both sites are subject to variation of C_D (Fig. 8). Mean values are C_D=0.13 at URB and C_D=0.15 at
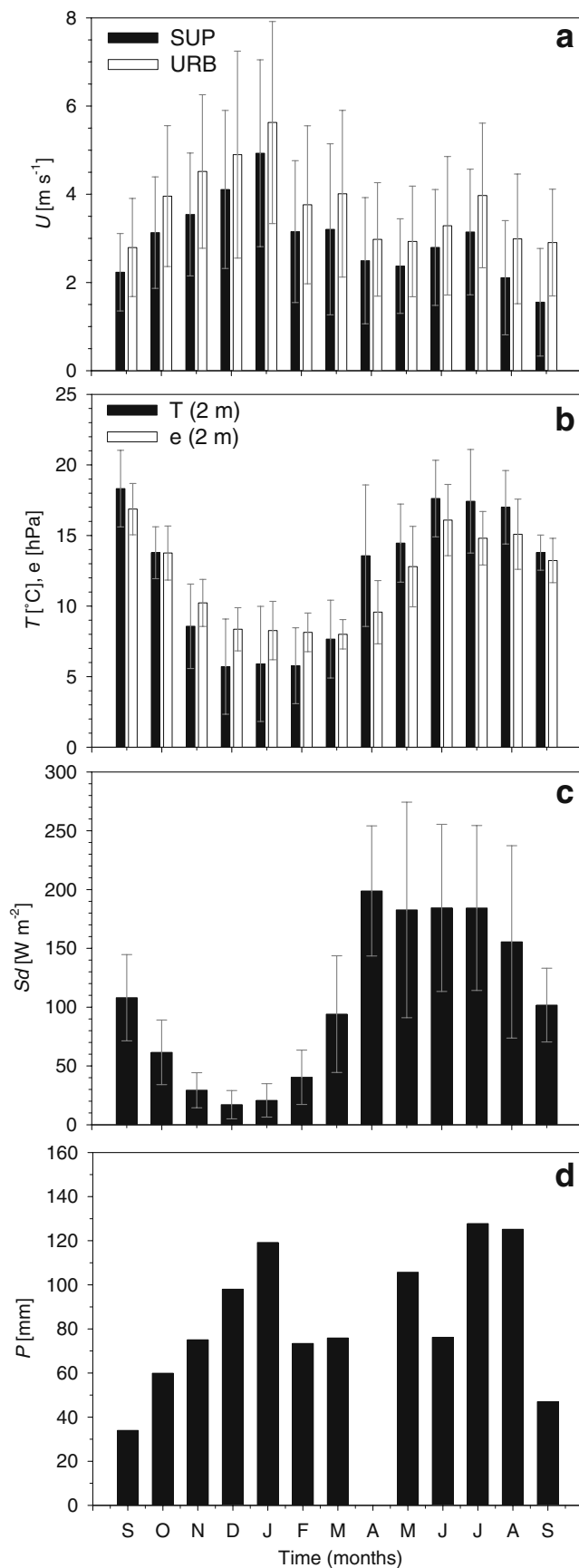
SUP, respectively. These averages correspond well to estimates from an empirical expression based on different urban observations as reported in Roth (2000). For the corresponding nondimensional building heights of the present sites (cf. Table 1), this expression results in $C_D=$ 0.14 (URB) and $C_D=0.16$ (SUP).

The exhibition centre situated in the south/southeast of SUP can be clearly detected in the data by maximum values of the drag coefficient. While some larger buildings situated in the northeast of URB are responsible for maxima of C_D, the remaining sectors are characterised by more comparable drag coefficients.

4.3.2 Standard deviations

To describe and compare the structure of turbulence above different surfaces, a number of observations on turbulence characteristics have been published during recent years. However, they mostly are restricted to short observational periods and limited ranges of atmospheric stability. Especially, data of urban turbulence characteristics under stable situations used to be scarce which makes the present data set important.
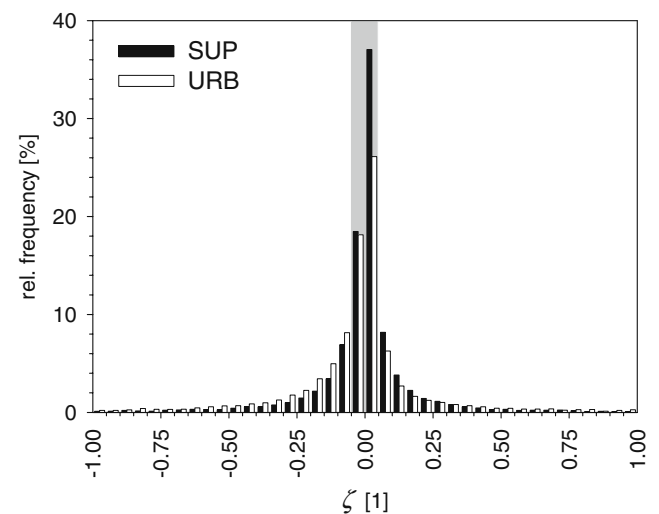

Fig. 5 Frequency distribution of the atmospheric stability parameter ζ binned into 0.05-ζ classes. The *grey shading* indicates the range of neutral stability as defined in the text. Only stabilities in the range from $-1 < \zeta < 1$ are shown in this plot; however, this accounts for more than 95% of data
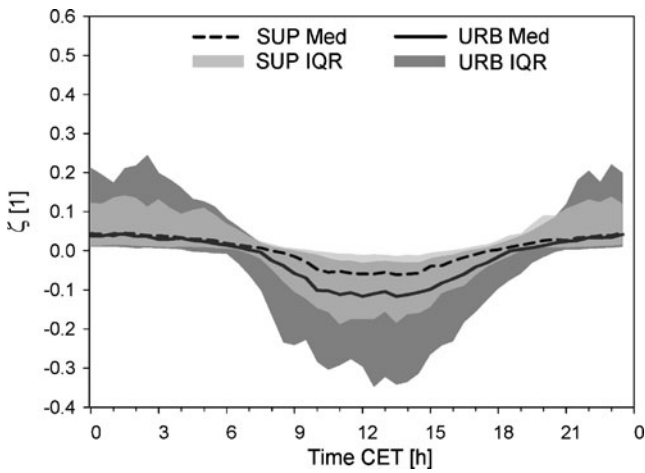
Fig. 6 Diurnal courses of the median (*Med*) of stability parameter ζ at URB and SUP for the entire study period (*CET* Central European Time). *Grey shadings* indicate the interquartile range (*IQR*) between 25th and 75th percentile, i.e. 50% of data lies within the range specified. Data is based on the entire study period

Fig. 8 Drag coefficient for neutral stability vs. wind direction sectors for SUP and URB. Wind directions are binned into 10°-classes. *Horizontal lines* are empirical fits according to Roth (2000) for z/z_H=2.05 (*solid line*, URB) and z/z_H=1.73 (*dashed line*, SUP)

Turbulence characteristics or normalised standard deviations of velocity are defined as the ratio of the standard deviations of wind vectors divided by friction velocity u_*. Within t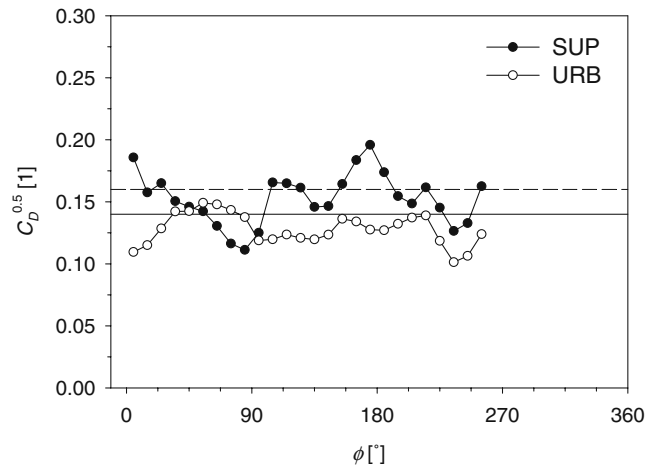he framework of the Monin Obukhov similarity theory, surface layer turbulence characteristics were shown to be a function of atmospheric stability (e.g. Kaimal and Finnigan 1994). However, due to the limited number of urban observations under stable stratification, the behaviour in these situations is still under debate.
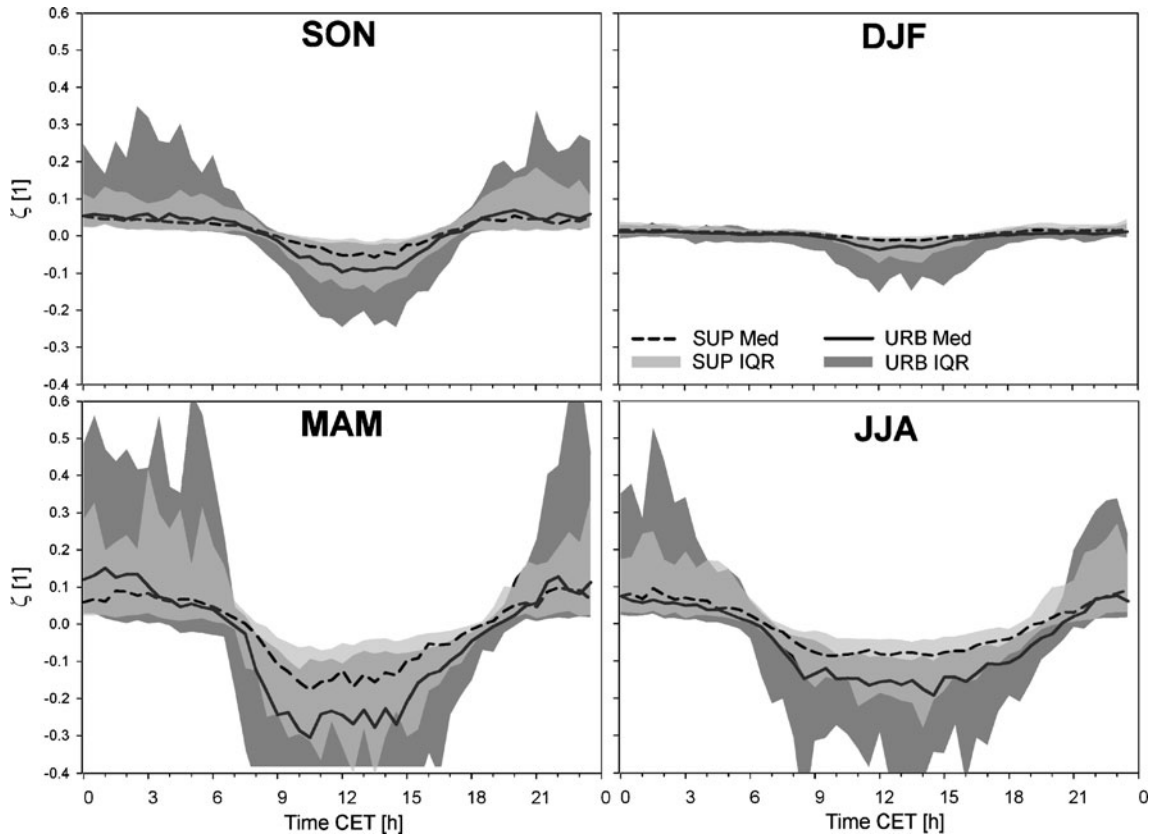

Fig. 7 Seasonal variation of the stability parameter ζ at both sites. (*SON* September, October, and November; *DJF* December, January, and February; *MAM* March, April, and May; *JJA* June, July, and August)

Table 3 Overview of constants in empirical fits according to Eq. 2 for unstable and stable stratification

		Roth (2000)			Al-Jiboori et al. (2002)		This Study				
		a	b	c	a	b	a	b	c	a	b
$\zeta < 0$	σ_u/u_*	1.98	0.33	0.56	1.75	1.80	1.98	0.53	0.57	1.93	1.28
	σ_v/u_*	1.64	2.84	0.30	1.60	2.10	2.03	0.32	0.86	1.96	1.37
	σ_w/u_*	1.12	2.48	0.33	1.22	1.05	1.33	1.53	0.62	1.29	1.52
$\zeta > 0$	σ_u/u_*	-	-	-	1.76	2.39	-	-	-	1.86	1.11
	σ_v/u_*	-	-	-	1.60	1.96	-	-	-	2.00	0.99
	σ_w/u_*	-	-	-	1.22	1.05	-	-	-	1.37	0.17

If constant c is not explicitly given in the table, it was set to 0.33. Both approaches (constant c, variable c) are provided for comparison to other studies
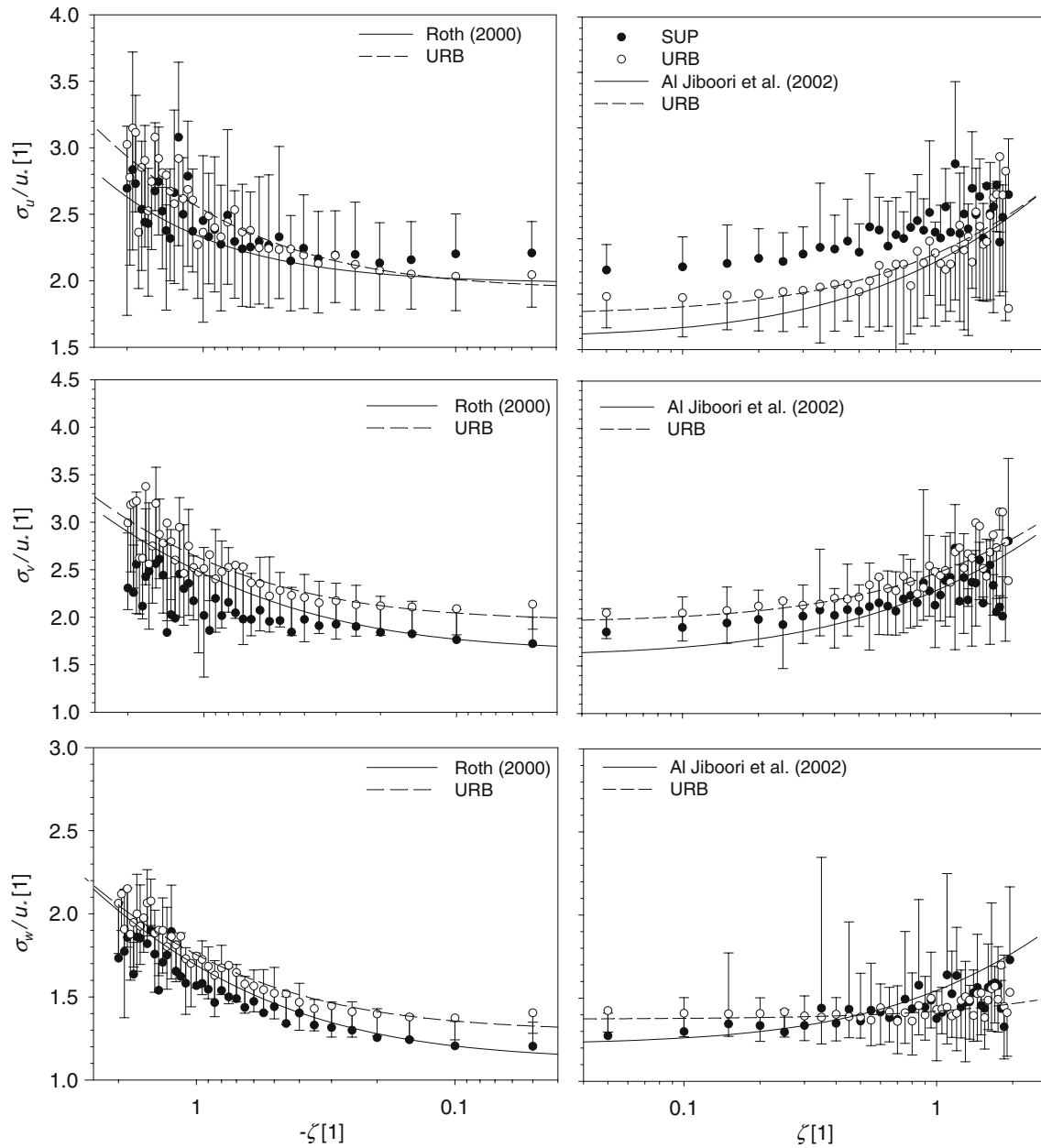

Fig. 9 Means of turbulence characteristics σ_i/u_* ($i=u, v, w$) vs. stability binned into 0.05-ζ classes for unstable ($-\zeta$, *left panel*) and stable (ζ, *right panel*) atmospheric stratification. *Error bars* indicate standard deviation. For reasons of clarity of the plots, only positive or negative standard deviations are indicated. Empirical fits are based on the data from URB and on literature data from Roth (2000) and Al-Jiboori et al. (2002)

In the unstable range ($\zeta < 0$), the behaviour can satisfyingly be fitted by a function of the form (e.g. Roth 2000)

$$\frac{\sigma_i}{u_*} = a(1 - b\zeta)^c \qquad (2)$$

with σ_i ($i = u$, v, w) the standard deviation of a wind vector in metre per second, u_* friction velocity in meter per second and a, b, and c empirical constants. The value of c was observed to be close to 0.33 and was set constant to this value in some observations (e.g. Al-Jiboori et al. 2002; Vesala et al. 2008). For comparison of observational data with different literature values, the data of this study will be fitted with both approaches, i.e. empirical fits with a constant value of $c = 0.33$ and a variable c (cf. Table 3).

Turbulence characteristics for both measurement sites in Essen have been calculated for different atmospheric stabilities (Fig. 9). In the unstable range, data follows empirical fits to urban data well and shows the general increase with increasing instability (Roth 2000). As documented by others (Zhang et al. 2001; Al-Jiboori et al. 2001), larger differences for the horizontal components in comparison to the vertical component are observable. Generally, departure from the Roth (2000) reference, data under neutral to slight unstable stratification, i.e. $\zeta > -0.4$, is visible. However, normalised standard deviations of velocity have been observed to vary in magnitude with observational site, i.e. comparison of absolute values is limited (Zhang et al. 2001). It is still under discussion whether normalised standard deviations are a function of surface roughness (Roth 2000). Differences in surface roughness depending on the direction of approaching flow (cf. Section 4.3.1) might attribute to the difference in magnitude of turbulence characteristics between sites. With stronger instability, data is very much in agreement with the reference data of Roth (2000). Empirical fits to the unstable and stable data at URB for comparison to other data from urban areas are provided in Table 3.

In the stable range ($\zeta > 0$), observations from homogeneous terrain reported the standard deviation to be relatively constant with increasing ζ (e.g. Nieuwstadt 1984; Al-Jiboori et al. 2002). While a rather constant behaviour of σ_w/u_* is observable at URB, the SUP ratio shows a slight increase with increasing stability. This agrees to empirical fits to stable data provided from the urban boundary layer in Beijing (Al-Jiboori et al. 2002). Both standard deviations of horizontal components show a similar increase with increasing stability of the surface layer at both sites (Fig. 9, right panel). This also was indicated in the stable data of Al-Jiboori et al. (2002). However, increases in the ratios with stability at URB and SUP, especially for the σ_w/u_* ratio, are not as strong as observed in their data. This is demonstrated by the smaller

values of the constant b in the empirical fits (Table 3) in comparison to the Al-Jiboori et al. (2002) data. However, it has to be noted that their stable data stretches to about $\zeta \approx 10$, while the majority of our observations ends at $\zeta = 1$ (cf. Fig. 5). Unfortunately, there is little observational evidence of stable data from other urban areas for comparison with our observations.
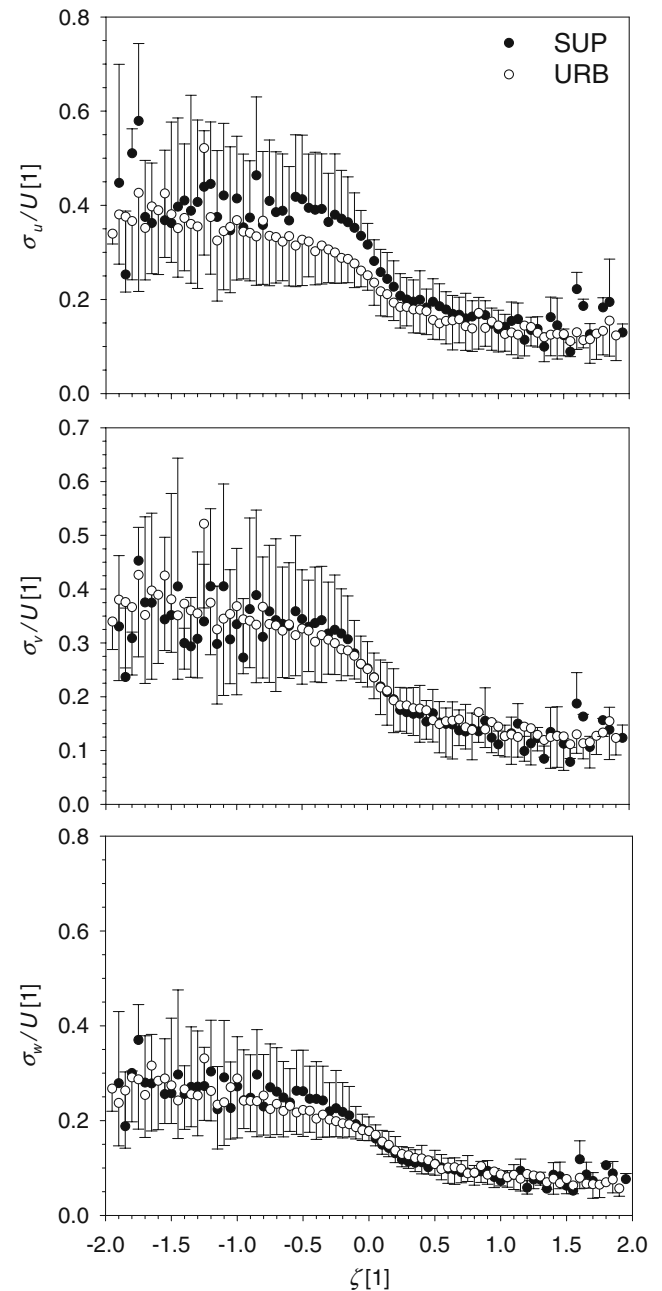

Fig. 10 Means of turbulence intensity σ_i/u ($i = u$, v, w) vs. stability binned into 0.05-ζ classes for unstable and stable atmospheric stratification. *Error bars* indicate standard deviation. For reasons of clarity of the plots, only positive or negative standard deviations are indicated

4.3.3 Turbulence intensity

Standard deviations of wind vectors divided by horizontal wind velocity can be interpreted as a measure of turbulence intensity (Roth 2000). Mean values for the different wind vectors under neutral stability found in this study are $\sigma_u/U=$ 0.33, $\sigma_v/U=0.26$, and $\sigma_w/U=0.18$ at SUP and $\sigma_u/U=0.26$, $\sigma_v/U=0.27$, and $\sigma_w/U=0.18$ at URB. These are in agreement to values reported by others (e.g. Roth 2000). The intensity of turbulence depends on atmospheric stability and decreases from unstable to neutral conditions at both sites (Fig. 10). In the stable range, turbulence intensity slightly decreases and shows somewhat constant behaviour from about $\zeta > 1$. Those more strongly stable situations are characterised by a general suppression of turbulence and wind shear.

4.4 Turbulent heat and momentum fluxes

The diurnal courses of heat and momentum fluxes at URB and SUP are relatively similar in their temporal evolution but they differ in magnitude (Fig. 11). With a maximum annual average heat flux at noon of 0.088 K m s^{-1} at URB (≈ 106 W m^{-2}), it is about 0.03 K m s^{-1} ($\approx$ 36 W m^{-2}) higher in comparison to SUP. Based on 1-year data of heat fluxes, URB is characterised by 30% higher fluxes. The larger kinematic heat fluxes are driven by stronger absorption of shortwave downward solar radiation and higher temperatures of the artificial surface cover at URB. The atmosphere reacts to stronger surface heating at the urban site with positive (upward directed) heat fluxes starting at around 0700 CET on average. At SUP, positive heat fluxes can be observed with a 1-h delay in comparison to URB (Fig. 11). After sunset, heat fluxes at URB remain positive for about 1.5 h after fluxes changed sign at SUP due to onset of surface cooling in the urban park. Negative surface heat fluxes during night time are generally small at both sites with nocturnal minima of

about -0.012 K m s^{-1} (≈ -15 W m^{-2}; SUP) and -0.010 K m s^{-1} (≈ -12 W m^{-2}, URB), respectively. However, the difference between both sites indicates SUP to experience stronger near-surface cooling during nighttime. Therefore, surface warming takes longer at SUP after sunrise. The intersite difference might be strengthened by some additional release of stored heat from the urban fabric at URB. Similar results of negative nocturnal heat fluxes were obtained in an urban energy balance model study by Harman and Belcher (2006). They discuss a lower heat capacity of the roof materials in comparison to urban canyons to be responsible for negative nocturnal sensible heat fluxes.

The general behaviour of heat flux differences between both sites is preserved throughout the year (Fig. 12). Maximum seasonal averages at noon are reached during MAM with 0.144 K m s^{-1} (≈ 173 W m^{-2}) at URB and 0.105 K m s^{-1} (≈ 126 W m^{-2}) at SUP. Higher fluxes during MAM in comparison to JJA are due to the persistence of a high-pressure system in April 2007 (cf. Section 4.1). However, the magnitude of fluxes is in accordance with flux estimates from other sites, e.g. Offerle et al. (2006) report maximum monthly averages of about 180 to 220 W m^{-2} (≈ 0.149 to 0.183 K m s^{-1}) for May and June from an urban site in Lodz, Poland. As stated before, the difference of noon heat fluxes at our sites can be estimated with about 30%. This also is in agreement to studies using more than one measurement site within a city (e.g. Grimmond et al. 2004; Kanda et al. 2006).

Heat fluxes during winter are generally small at both sites reaching noon maxima of around 0.020 K m s^{-1} ($\approx$ 24 W m^{-2}) at SUP and 0.035 K m s^{-1} (≈ 42 W m^{-2}) at URB. A fraction of this 0.015 K m s^{-1} (≈ 18 W m^{-2}) intersite difference might be related to an effect of increased anthropogenic heating in the vicinity of URB. Generally, intersite differences are larger in winter, e.g. the daytime average ratio of URB/SUP for Q_H is about a factor 2 during winter and 1.5 during the summer season. Offerle et al.

Fig. 11 Average diurnal courses of kinematic and sensible heat fluxes at both sites for the 1-year measurement period. *Positive values* of Q_H represents upward directed heat fluxes, and *negative signs* indicate downward directed fluxes. S_d indicates the average diurnal course of shortwave downward radiation at HSW
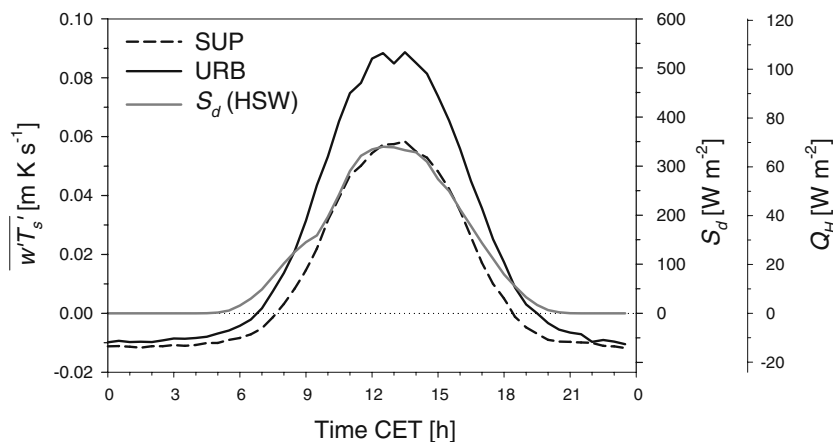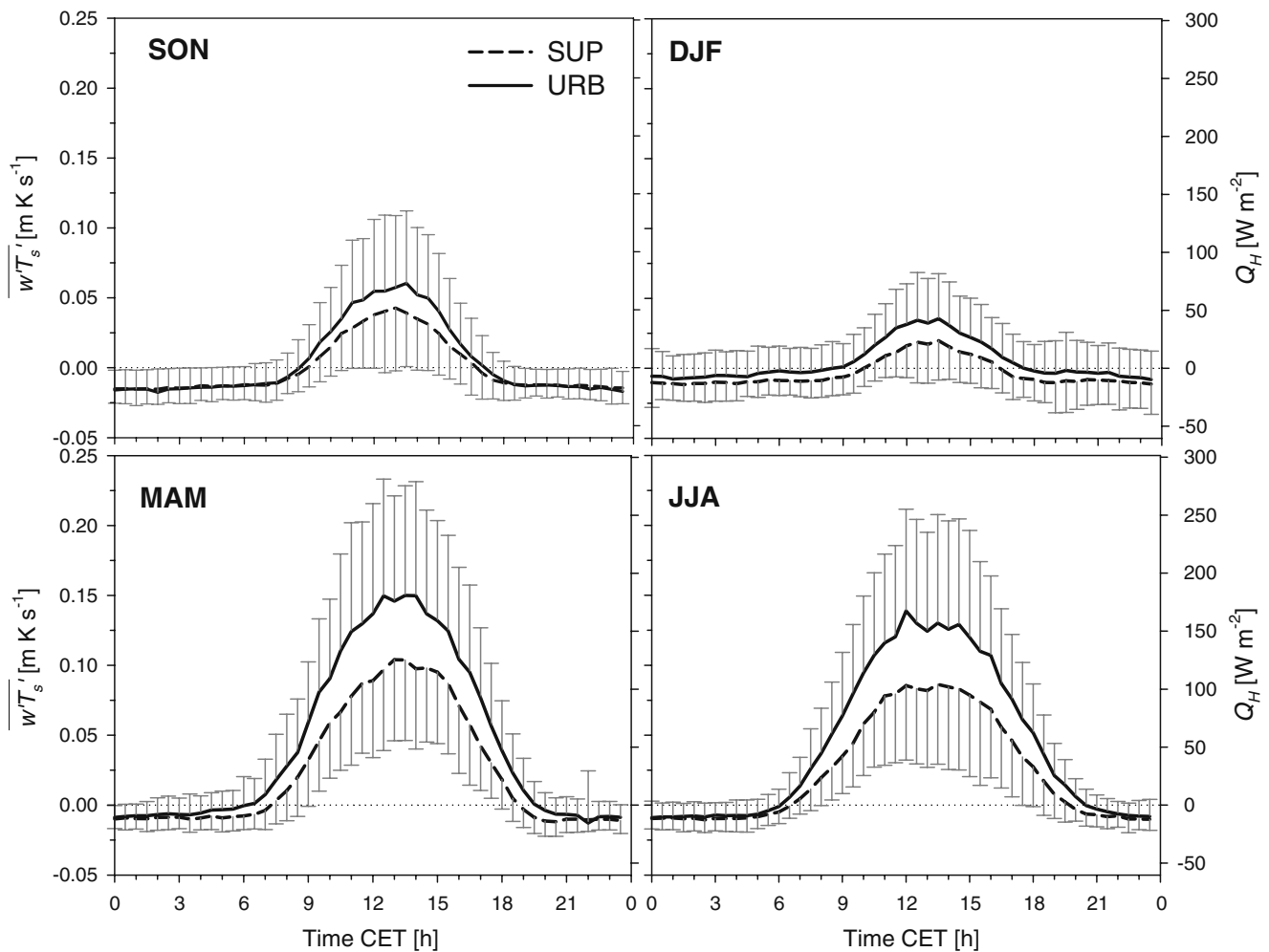
Fig. 12 Seasonally averaged diurnal courses of kinematic and sensible heat fluxes during the 1-year study period. *Error bars* indicate standard deviations. For reasons of clarity of the plots, only positive or negative standard deviations are indicated

(2005) found that the wintertime anthropogenic heat flux during noon reaches a magnitude of about 40% of Q_H on average. This estimate roughly corresponds to the intersite difference found in this study.

The temporal evolution of vertical transport of momentum (momentum flux) is depicted in Fig. 13. During daytime, values peak around noon. However, values at both sites are separated by about 18% and reach similar magnitudes during nighttime. Based on 1 year of data, the difference between sites is about 6%. Seasonally, this behaviour is more or less conserved. Largest differences occur during periods of highest horizontal wind velocity, namely in the fall and winter period (data not shown here).

5 Summary and conclusions

Turbulence measurements were performed during a 1-year period at two sites in Essen, Germany to assess similarities and differences in urban surface layer characteristics. The
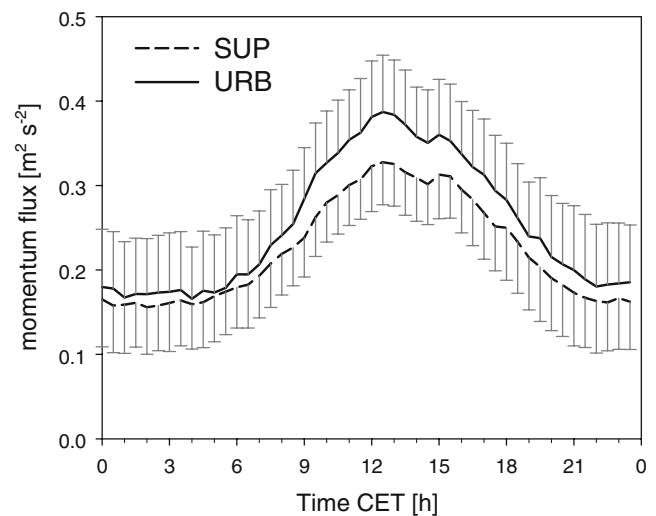

Fig. 13 Average diurnal courses of momentum fluxes at both sites for the 1-year measurement period. *Vertical error bars* indicate standard deviations. For reasons of clarity of the plots, only positive or negative standard deviations are indicated

data were analysed for intersite variability of atmospheric stability, turbulence characteristics, and surface heat fluxes. Measurements were taken at two spots with different fractions of surface cover and surface morphology around sites to verify effects on turbulent flow.

Our analysis documented that turbulence characteristics represented observations and empirical fits to data from other urban experiments satisfyingly. Although showing comparable behaviour with varying stability of the atmosphere, deviations in the turbulence characteristics (standard deviations, turbulence intensity) between the sites occurred. These are attributed to differences in roughness and surface cover around the sites.

Distinctions in atmospheric stability and surface heat fluxes were observed to be related to the different physical parameters of the surfaces at both sites. These allow for deviation in the time evolution as well as in the magnitude of surface heating at both sites. URB generally shows typical urban features; increased surface heating leads to higher surface heat fluxes in comparison to SUP. Also the temporal evolution in the course of the day is affected in a way that heat fluxes react faster to surface heating after sunrise and remain positive for about 1.5 h after fluxes changed sign at SUP due to onset of surface cooling in the urban park. The different arrangement of surface cover has distinct influence on average heat fluxes and during different seasons of the year.

It can be concluded that turbulence characteristics measured at different flux sites within the urban boundary layer may be characterised by general similarities but are still—to a certain amount—influenced by the heterogeneous urban flux footprint. This has to be taken into account when urban flux estimates from single sites are incorporated into applications such as dispersion modelling and pollution forecasts.

References

Al-Jiboori M, Yumao X, Yongfu Q (2001) Turbulence characteristics over complex terrain in west China. Boundary-Layer Meteorol 101:109–126

Al-Jiboori M, Xu Y, Qian Y (2002) Local similarity relationships in the urban boundary layer. Boundary-Layer Meteorol 102:63–82

Arnfield J (2003) Two decades of urban climate research: a review of turbulence, exchanges of energy and water, and the urban heat island. Int J Climatol 23:1–26

Christen A (2005) Atmospheric turbulence and surface energy exchange in urban environments—results from the Basel Urban Boundary Layer Experiment (BUBBLE). Stratus 11, University of Basel, p 140

Christen A, Vogt R (2004) Energy and radiation balance of a central European city. Int J Climatol 24:1395–1421

Foken T (2006) Angewandte Meteorologie - Mikrometeorologische Methoden. Springer, Heidelberg, 325pp

Garratt JR (1992) The atmospheric boundary layer. Cambridge University Press, Cambridge, 316pp

Grimmond CSB, Oke TR (1999) Aerodynamic properties of urban areas derived from analysis of surface form. J Appl Meteorol 38:1262–1292

Grimmond CSB, Oke TR (2000) Heat fluxes and stability in cities, Third Symposium on the Urban Environment, American Meteorological Society, 14.-18.08.2000, Davis, 28–29

Grimmond CSB, Salmond JA, Oke TR et al (2004) Flux and turbulence measurements at a densely built-up site in Marseille: heat, mass (water and carbon dioxide), and momentum. J Geophys Res 109(D24101 doi:10.1029/2004JD004936)

Harman IN, Belcher SE (2006) The surface energy balance and boundary layer over urban street canyons. Q J Roy Meteorol Soc 132:2749–2768

Kaimal JC, Finnigan JJ (1994) Atmospheric boundary layer flows—their structure and measurements. Oxford University Press, New York, Oxford

Kanda M, Moriwaki R, Kasamatsu F (2006) Spatial variability of both turbulent fluxes and temperature profiles in an urban roughness layer. Boundary-Layer Meteorol 121:1–12

Kastner-Klein P, Rotach M (2004) Mean flow and turbulence characteristics in an urban roughness sublayer. Boundary-Layer Meteorol 111:55–84

Kuttler W (2008) The urban climate—basic and applied aspects. In: Marzluff JM et al (ed.), Urban ecology—an international perspective on the interaction between humans and nature. Springer, pp. 233–248

Mahrt L, Sun J, Blumen W et al (1998) Nocturnal boundary-layer regimes. Boundary-Layer Meteorol 88:255–278

Müller-Westermeier G (1996) Klimadaten von Deutschland. Zeitraum 1961–1990. Selbstverlag des Deutschen Wetterdienstes, Offenbach am Main.

Nemitz E, Hargreaves KJ, McDonald AG et al (2002) Micrometeorological measurements of the urban heat budget and CO2 emissions on a city scale. Env Sci Tech 36:3139–3146

Newton T, Oke TR, Grimmond CSB et al (2007) The suburban energy balance in Miami, Florida. Geogr Annaler A 89:331–347

Nieuwstadt FTM (1984) The turbulent structure of the stable nocturnal boundary layer. J Atmos Sci 41:2202–2216

Offerle B, Grimmond CSB, Fortuniak K (2005) Heat storage and anthropogenic heat flux in relation to the energy balance of a central European city centre. Int J Climatol 25:1405–1419

Offerle B, Grimmond CSB, Fortuniak K et al (2006) Temporal variations in heat fluxes over a central European city centre. Theor Appl Climatol 84:103–115

Oke TR (1988) The urban energy balance. Prog Phys Geography 12:471–508

Oke TR, Spronken-Smith RA, Jauregui E et al (1999) The energy balance of central Mexico City during the dry season. Atmos Environ 33:3919–3930

Piringer M, Grimmond CSB, Joffre SM et al (2002) Investigating the surface energy balance in urban areas—recent advantages and future needs. Water Air Soil Poll Focus 2:1–16

Rotach MW, Vogt R, Bernhofer C et al (2005) BUBBLE—an urban boundary layer meteorology project. Theor Appl Climatol 81:231–261

Roth M (2000) Review of atmospheric turbulence over cities. Q J Royal Meteorol Soc 126:941–990

Schmid HP (1994) Source areas for scalars and scalar fluxes. Boundary-Layer Meteorol 67:293–318

Schmid HP (1997) Experimental design for flux measurements: matching scales of observations and fluxes. Agri Forest Meteorol 87:179–200

Spronken-Smith R (2002) Comparison of summer and winter-time suburban energy fluxes in Christchurch, New Zealand. Int J Climatol 22:979–992

Stull RB (1988) An introduction to boundary layer meteorology. Atmospheric sciences library, Kluwer Academic, Dordrecht

UN-Habitat (2006) State of the world's cities 2006/2007. The millennium development goals and urban sustainability (UN Habitat), Nairobi

Vesala T, Järvi L, Launiainen S et al (2008) Surface–atmosphere interactions over complex urban terrain in Helsinki, Finland. Tellus B 60:188–199

Vogt R, Christen A, Rotach MW (2006) Temporal dynamics of CO_2 fluxes and profiles over a Central European city. Theor Appl Climatol 84:117–126

Weber S, Weber K (2008) Coupling of urban street canyon and backyard particle mass and number concentrations. Meteorol Z 17:251–261

Weber S, Kuttler W, Weber K (2006) Flow characteristics and particle mass and number concentration variability within a busy urban street canyon. Atmos Environ 40:7565–7578

Zhang H, Chen J, Park SJ (2001) Turbulence structure in unstable conditions over various surfaces. Boundary-Layer Meteorol 100:243–261